

Photon rings in the metamaterial analog of a gravitomagnetic monopole

A. Parvizi ^(a,b,c) *, H. Forghani-Ramandy ^{(a)†}, E. Rahmani ^{(a)‡} and M. Nouri-Zonoz ^{(a)§}

*(a):Department of Physics, University of Tehran,
North Karegar Ave., Tehran 14395-547, Iran.*

*(b):Institute for studies in theoretical physics and
mathematics (IPM), Farmanieh, Tehran, Iran.*

*(c): Institute for Theoretical Physics,
Faculty of Physics and Astronomy, University of Wroclaw,
pl. M. Borna 9, 50-204 Wroclaw, Poland.*

Abstract

After studying null geodesics in the equatorial plane in NUT spacetime, we show that there are unstable photon rings in this plane. Next we transform the metric of this plane to the isotropic coordinates and introduce its equivalent index of refraction. Using the analog gravity ideas we assign this index of refraction to a metamaterial analog of this plane, and by ray-tracing simulation find its photon rings. Furthermore, we employ wave optics to solve Maxwell's equations numerically for electromagnetic waves within an inhomogeneous medium characterized by the same index of refraction. Further we investigate the optical behaviour of this medium in response to the radiation from an electric dipole.

* Electronic address: aliasghar.parvizi@uwr.edu.pl

† Electronic address: hasan.forghani@ut.ac.ir

‡ Electronic address: elnaz.rahmani@ut.ac.ir

§ Electronic address: nouri@ut.ac.ir (Corresponding author)

I. INTRODUCTION

Metamaterial analogs of different spacetimes, based on their optical characteristics, have already been studied in the literature, specially after the introduction of the transformation optics [1, 2]. One of the main features of metamaterials, which was utilized through transformation optics, was the great ability in controlling their optical properties by assigning them with the desired optical parameters. Linking this with the behaviour of light rays in the exact solutions of Einstein field equations, through the assigned index of refraction, one can in principle design metamaterial analogs of these spacetimes mimicking their interesting optical behavior. These include the formation of photon spheres in the ray tracing simulations of metamaterial analogs of static spherically symmetric spacetimes [3], and wave optics simulations of light propagation in the metamaterial analogs of different spacetimes [4–8]. Based on the same analogy people have investigated properties of the so-called optical black holes in their dielectric and metamaterial analogs [9–11].

One of the interesting exact solutions of the Einstein field equations which has not been studied in this context is the NUT solution [12]. This solution, interpreted as the gravitational analog of a magnetic monopole, or the so called gravitomagnetic monopole, has a number of exotic properties [13]. These properties, originated from its Dirac-type string singularity, featured NUT spacetime as “*a counter example to almost anything*” [14]. NUT spacetime is a stationary spacetime, and in the case of stationary spacetimes, unlike the static spherically symmetric spacetimes, one can not transform the corresponding metric to an isotropic coordinates to be able to assign an index of refraction to the whole spacetime. On the other hand in the case of NUT solution, one could restrict the study to the equatorial plane $\theta = \pi/2$ which could be transformed to the isotropic coordinates, and be assigned with an index of refraction. We will show that the the main optical feature in this plane, i.e the presence of *photon rings* as unstable orbits could be implemented in its metamaterial analog by assigning the metamaterial with the plane’s index of refraction. The closest case to NUT spacetime which is both stationary and has two parameters, as well as possessing equatorial photon rings, is the Kerr spacetime [15], so we will compare our results with those obtained in the Kerr case and its metamaterial analog [15].

This opto-geometric relation provides us with the possibility of testing the optical properties of the most exotic solutions of Einstein field equations, namely black holes, in laboratory

settings. On the other hand one can design metamaterial devices with interesting and unique optical features that utilize optical features in the corresponding black hole spacetime, for instance optical concentrator proposed in [16] or Hawking radiation in an optical analogue of the black-hole horizon [17].

The outline of the paper is as follows. In the next section we give a brief review of the NUT spacetime and its interesting features. In section III we will discuss the presence of photon rings in equatorial NUT spacetime, and transform its metric to isotropic coordinates, thereby assigning it with an index of refraction. In section IV we will employ the ray-tracing simulation in the metamaterial analogs of the equatorial NUT and pure NUT spacetimes, and find their photon rings, and study the effect of NUT factor on their optical properties. In section V we present a more visual demonstration of the photon ring simulations by projecting them on the embedding diagram of the equatorial NUT plane. In Section VI, we consider an extension of the NUT spacetime, the so-called *charged* NUT spacetime, which contains electric charge as its third parameter. Calculating its equivalent index of refraction, we employ a wave optics approach to explore the optical features of its metamaterial analog. We show that the inclusion of three parameters provides enhanced control over the radii of photon rings in the corresponding metamaterial analog, and consequently facilitate the design of optical devices based on them.

Conventions: In what follows we will use natural units in which $c = G = 1$, and the metric signature is given by (1,-1,-1,-1).

II. A BRIEF REVIEW OF NUT SPACETIME

NUT spacetime in Schwarzschild-like coordinates is given by the following metric [18],

$$ds^2 = f(r)(dt - 2l \cos \theta d\phi)^2 - \frac{dr^2}{f(r)} - (r^2 + l^2)d\Omega^2 \quad (1)$$

with

$$f(r) = \frac{r^2 - 2mr - l^2}{r^2 + l^2} \quad (2)$$

in which m and l are the mass and NUT (magnetic mass) parameters respectively. For $l = 0$ we recover the Schwarzschild metric, whereas for $m = 0$ unlike the Kerr case, we do not find flat spacetime in an exotic coordinate, but the so called *pure* NUT spacetime which is a one-parameter stationary spacetime.

Although, the NUT spacetime is manifestly axisymmetric with the axis along the *string singularity* at $\theta = 0, \pi$, its curvature invariants are spherically symmetric. This is due to the fact that one could transform the above metric, using the time coordinates

$$t_N = t - 2l\phi \quad (3)$$

$$t_S = t + 2l\phi \quad (4)$$

to the following two forms respectively

$$ds^2 = f(r) \left(dt_N + 4l \sin^2 \frac{\theta}{2} d\phi \right)^2 - \frac{dr^2}{f(r)} - (r^2 + l^2) d\Omega^2 \quad (5)$$

$$ds^2 = f(r) \left(dt_S - 4l \cos^2 \frac{\theta}{2} d\phi \right)^2 - \frac{dr^2}{f(r)} - (r^2 + l^2) d\Omega^2, \quad (6)$$

where in the first form there is a singularity only in the half-axis $\theta = \pi$, whereas in the second form the singularity is in the half-axis $\theta = 0$. This in principle shows that one could change the direction of the half-axis singularity to any other direction. Using this freedom Misner showed that one could remove the string singularity by covering the whole manifold with two different coordinate patches for the northern ($0 < \theta < \pi/2$), and the southern ($\pi/2 < \theta < \pi$) regions. For $r = \text{constant}$ hypersurface, these are sloid tori with topology $S^1 \times E^2$, sharing a boundary at $\theta = \pi/2$ which is a torus ($S^1 \times S_t$) [13]. To achieve this it is noted from (3)-(4), that the identification of time at the boundary leads to

$$t_N = t_S - 4l\phi \quad (7)$$

showing the angular character of either of the time coordintes. Consequently, by the single-valuedness of the ϕ coordinate, it leads to

$$t_{N/S} = t_{N/S} \pm 8\pi l. \quad (8)$$

In other words the sigularity-free form of the metric comes at the price of introducing a periodic time, but this shows that one could in principle find a singularity-free form of the metric which justifies the *physical* spherical symmetry of the NUT hole, despite its mathematically evident axially symmetric metric.

Taking the radial coordinate $0 < r < \infty$, there is a coordinate singularity in NUT spacetime at $r_H = m + (m^2 + l^2)^{1/2}$ (where $f(r) = 0$) as the NUT horizon ¹, which unlike the

¹ In its maximal extension where $-\infty < r < \infty$ there are coordinate singularities in NUT spacetime at $r_{\pm} = m \pm (m^2 + l^2)^{1/2}$ corresponding to two distinct NUT regions for $r > r_+$ and $r < r_-$ with $f(r) > 0$ separated by the so called Taub region $r_- < r < r_+$ where $f(r) < 0$ [19].

Schwarzschild horizon, does not hide a singularity at $r = 0$, so we may call the NUT spacetime either a NUT *hole* or a NUT *black hole*.

Because of its Dirac-type singularity, the NUT space is interpreted as the spacetime of a mass endowed with a gravitomagnetic monopole charge (the NUT parameter). This justifies its spherical symmetry despite its axisymmetric appearance [20, 21]. Bonnor gave another interpretation of NUT spacetime in terms of a semi-infinite massless source of angular momentum [22].

III. PHOTON RINGS IN THE EQUATORIAL NUT SPACETIME IN ISOTROPIC COORDINATES

The null geodesics of NUT spacetime have already been studied in the literature, with an emphasis on light bending [23]-[24]. Here we are interested in its photon rings in the equatorial plane, and in *isotropic* coordinates. To this end we restrict our attention to the line element of the subspace $\theta = \pi/2$, namely

$$ds^2 = f(r)dt^2 - \frac{dr^2}{f(r)} - (r^2 + l^2)d\phi^2, \quad (9)$$

in which the metric function $f(r)$ is defined in (2). The Lagrangian for the geodesics of the NUT spacetime is

$$2\mathcal{L} = f(r)\dot{t}^2 - \frac{\dot{r}^2}{f(r)} - (r^2 + l^2)\dot{\phi}^2 \quad (10)$$

where $\cdot \equiv d/d\lambda$ and λ is an affine parameter along the null geodesics. Since the Lagrangian is independent of t and ϕ , we have the following two first integrals from the Euler-Lagrange equations,

$$f(r)\dot{t} = E \quad (11)$$

$$(r^2 + l^2)\dot{\phi} = L \quad (12)$$

representing the energy and angular momentum respectively. Also for null geodesics we have $ds^2 = 0 = \mathcal{L}$ leading to

$$f(r)\dot{t}^2 - \frac{\dot{r}^2}{f(r)} - (r^2 + l^2)\dot{\phi}^2 = 0 \quad (13)$$

Unstable circular null geodesics forming at radial coordinate $r = r_c$, are given by $\dot{r} = 0$ in the above equation, which along with equations (11)-(12) leads to

$$\frac{\dot{t}}{\dot{\phi}} = \frac{L}{E} \equiv b_c \quad (14)$$

in which b_c by definition is the impact parameter for rays coming from infinity to be trapped on the photon ring at $r = r_c$. Replacing this back into equation (13) for a photon ring we end up with

$$(r_c^2 + l^2)^2 = (r_c^2 - 2mr_c - l^2)b_c^2, \quad (15)$$

other equation governing the unstable circular photon rings can be derived by taking the derivative of the above equation with respect to r_c , which yields

$$4r_c(r_c^2 + l^2) = (2r_c - 2m)b_c^2, \quad (16)$$

then we read impact parameter b_c as follows

$$b_c = \sqrt{\frac{2r_c(r_c^2 + l^2)}{r_c - m}} \quad (17)$$

Replacing this back into equation (15), we find the following 3-rd order equation for the radial coordinate of the photon ring

$$r_c^3 - 3mr_c^2 - 3l^2r_c + ml^2 = 0 \quad (18)$$

with the negative discriminant $\Delta = -l^2(l^2 + m^2)^2$, all the three roots are real and unequal,

$$r_c = m + 2\sqrt{l^2 + m^2} \cos\left(\frac{1}{3} \tan^{-1}\left(\frac{l}{m}\right)\right), \quad (19)$$

$$r_c^\pm = m \pm \sqrt{l^2 + m^2} \left(\sqrt{3} \sin\left(\frac{1}{3} \tan^{-1}\left(\frac{l}{m}\right)\right) \mp \cos\left(\frac{1}{3} \tan^{-1}\left(\frac{l}{m}\right)\right) \right). \quad (20)$$

One could see that only the first solution gives a radius larger than that of outer horizon r_H^+ , and at the same time for $l = 0$ reduces to the corresponding value for the photon sphere in Schwarzschild black hole, $r_{ps} = 3m$ [3]. The other two solutions, for all values of l and m are inside the horizon, and are not either physically acceptable, or suitable for our simulation purposes which only cover the exterior of the NUT hole. Also it is noted that both $\pm l$ give the same solution as expected from (18). This is another difference compared to the Kerr case in which the $\pm a$ give two different photon rings as the direct, and retrograde orbits in its equatorial plane [15].

Now that we have the photon ring radius in Schwarzschild-type coordinates, we can transform it to the isotropic coordinates by transforming the equatorial NUT metric to the same coordinates. The equatorial NUT metric (9) can be transformed into the isotropic coordinates by the following transformation,

$$r = \frac{(2\rho + m)^2 + l^2}{4\rho} \quad (21)$$

leading to

$$ds^2 = f(r(\rho)) dt^2 - F(\rho) dl_f^2, \quad (22)$$

$$f(r(\rho)) = \frac{(4\rho^2 - l^2 - m^2)^2}{l^4 + 2l^2(m^2 + 4m\rho + 12\rho^2) + (m + 2\rho)^4}, \quad (23)$$

$$F(\rho) = \frac{1}{\rho^2} \left[l^2 + \left(\left(\frac{l}{2\rho} \right)^2 + \left(1 + \frac{m}{2\rho} \right)^2 \right)^2 \right] \quad (24)$$

where $dl_f^2 = d\rho^2 + \rho^2 d\phi^2$ is the spatial line element in flat spacetime, and the corresponding refractive index for the equatorial NUT will be [3],

$$n_{\text{NUT}}(\rho) = \left[\frac{F(\rho)}{f(r(\rho))} \right]^{\frac{1}{2}} = \frac{1}{4} \frac{l^4 + 2l^2(m^2 + 4m\rho + 12\rho^2) + (m + 2\rho)^4}{\rho^2(4\rho^2 - l^2 - m^2)} \quad (25)$$

Locations of the horizon ρ_H^+ , and the photon ring ρ_c in isotropic coordinates are given respectively by

$$\rho_H^+ = \frac{1}{2} \sqrt{m^2 + l^2}. \quad (26)$$

and

$$\begin{aligned} \rho_c = & \sqrt{l^2 + m^2} \cos \left(\frac{1}{3} \tan^{-1} \left(\frac{l}{m} \right) \right) \\ & + \frac{1}{2} \sqrt{\left((l^2 + m^2) + 2(l^2 + m^2) \cos \left(\frac{2}{3} \tan^{-1} \left(\frac{l}{m} \right) \right) \right)}. \end{aligned} \quad (27)$$

The impact parameter of the rays forming the photon ring b_c , being a constant of motion, is given by replacing for r_c from (19) in (17), which is a function of m and l as follows,

$$b_c = \sqrt{\frac{2 \left[m + 2\sqrt{l^2 + m^2} \cos \left(\frac{1}{3} \tan^{-1} \left(\frac{l}{m} \right) \right) \right] \left[\left(m + 2\sqrt{l^2 + m^2} \cos \left(\frac{1}{3} \tan^{-1} \left(\frac{l}{m} \right) \right) \right)^2 + l^2 \right]}{2\sqrt{l^2 + m^2} \cos \left(\frac{1}{3} \tan^{-1} \left(\frac{l}{m} \right) \right)}}. \quad (28)$$

Now having both ρ_c and b_c we can carry on with the simulation of photon rings. As pointed out previously what we are going to simulate in the next section, is the metamaterial analog of the outer region (i.e $\rho > \rho_H^+$) of the NUT equatorial plane. Obviously the assigned index of refractions (25) is also restricted to the same region.

IV. RAY-TRACING SIMULATION OF PHOTON RINGS

Simulation of light ray trajectories in the metamaterial analog of the NUT equatorial plane with the index of refraction (25) could be carried out in the same way as done for the

Parameters	ρ_H	b_c	ρ_c (from Equation)	ρ_c (from Simulation)
$m = 2, l = 0.5$	1.03077640640441	10.5699133286824	3.83210337020209	3.83210357449516
$m = 2, l = 2$	1.41421356237309	12.7725658645123	5.06959259652961	5.06959279537673
$m = 2, l = 6$	3.16227766016837	22.7225470527276	10.6275704238575	10.6275707546622
$m = 0, l = 2$	1	5.65685424949238	3.14626436994197	3.14626448629901
$m = 0, l = 6$	3	16.9705627484771	9.43879310982591	9.43879340740875

TABLE I: The photon ring locations were determined through simulations and exact calculations for different values of mass and NUT parameters. These photon rings are formed by a light beam originating from an initial distance of $\rho_0 = 72 \rho_{Sch} = 36m$.

metamaterial analog of the Schwarzschild black hole in [3]. This is so because the equatorial line elements in both cases basically entail the same type of geometry. So we use the same relation between the index of refraction and the critical angle the rays should make with the radial direction (i.e angle of the cone of avoidance) to form the photon ring starting from any given isotropic radial coordinate namely,

$$\sin \Theta_{cr} = \frac{b_c}{\rho n(\rho)}. \quad (29)$$

Numerical values of mass and NUT factor used in our simulations, leading to different photon rings in both equatorial NUT and pure NUT ($m = 0$) holes, are presented in table I. This table also includes the values for the photon ring positions obtained both from its exact value (27), and that obtained from the simulation. Table I reveals that the simulation results closely match the exact values, with an agreement at the order of approximately $\sim 10^{-6}$. Achieving this level of precision for the location of photon rings required the light rays to complete at least five orbits around the hole. To attain even greater precision, we must fine-tune the impact parameter b_c , allowing the rays to complete more than five orbits. In the subsequent discussions, we will delve into the simulation results for both the NUT and pure NUT spacetimes.

A. The NUT hole

The results of simulation for a congruence of light ray trajectories in the metamaterial analog of the equatorial NUT hole ($m, l \neq 0$), leading to the formation of photon rings, are shown in Figs. 1a and 1b for different values of parameters m and l . As is evident, we

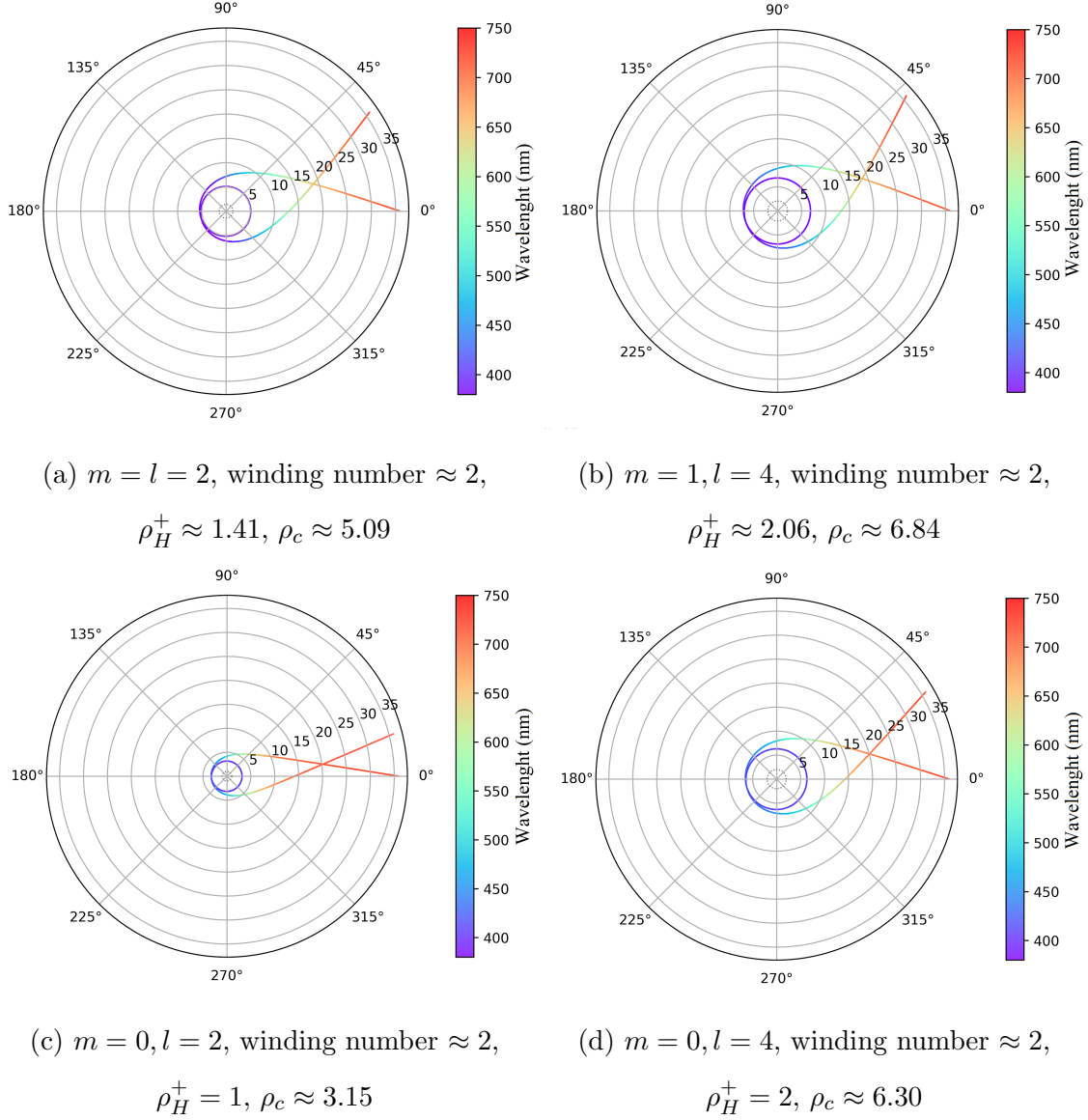


FIG. 1: Light ray trajectories in the metamaterial analog of the equatorial NUT (a,b), and pure NUT (c,d) holes, and the formation of photon rings (blue and purple circles).

Distances are scaled to $m/2$.

can change the locations of horizon, and photon rings by changing these parameters. The color palettes in Fig. 1 represent the strength of the refractive index, and the computed wavelength, which are governed by the relation $\frac{n(\rho_2)}{n(\rho_1)} = \frac{\lambda(\rho_1)}{\lambda(\rho_2)}$. In the special case of a NUT hole with $m = l = 2$, simulation details, and characteristics of the photon ring are tabulated in table II. These include the employed precision of the critical angle Θ_{cr} , the number of full rotations of rays around the hole (winding number), photon ring position (ρ_c), and the

Precision of the critical angle	Winding Number	Position of the photon ring	$\rho_c^{theory} - \rho_c^{simulation}$
10^{-4}	1.5	5.22173200935687	0.152139413
10^{-5}	2.2	5.08359798965296	0.014005393
10^{-7}	2.9	5.07123175414464	0.001639158
10^{-10}	3.7	5.06971567460091	0.000123078
10^{-12}	4.7	5.0695950000655	0.00000240354
10^{-17}	5.5	5.06959282392176	0.000000227392

TABLE II: The photon ring characteristics of a metamaterial analog of a NUT hole with $m = l = 2$ (depicted in Fig. 1a).

difference between photon ring positions obtained from the theory and the simulation.

B. The pure NUT hole

In this subsection, our attention is directed towards the pure NUT case, allowing us to explore the exclusive impact of the NUT factor on the optical properties of the corresponding metamaterial analogs. The simulation results for ray trajectories in a metamaterial analog of a pure NUT hole, characterized by NUT factors $l = 2$ and $l = 4$, are depicted in Figs. 1c and 1d. Comparing these figures with those for a NUT hole with a non-vanishing mass, Figs. 1a and 1b, could give us a better insight into the optical effects of the NUT factor l . For example comparing Figs. 1d with 1b, we observe that both cases have almost the same horizons with differing photon ring radii of about $\sim m/4$, while the corresponding refractive indices at the same radii differ notably. Thus, as expected, we find that the presence of a mass parameter increases the refractive index at a given radius, and consequently leads to a decrease in the light wavelength. In contrast, the NUT factor l primarily affects the horizon, and the photon ring positions, with minimal impact on the refractive index and light wavelengths.

Another noteworthy point is that in all our simulations in Fig. 1, the maximum winding number for the photon rings is 2, while it is possible to achieve higher winding numbers by increasing computational precision and cost, as shown for the special case of a NUT hole

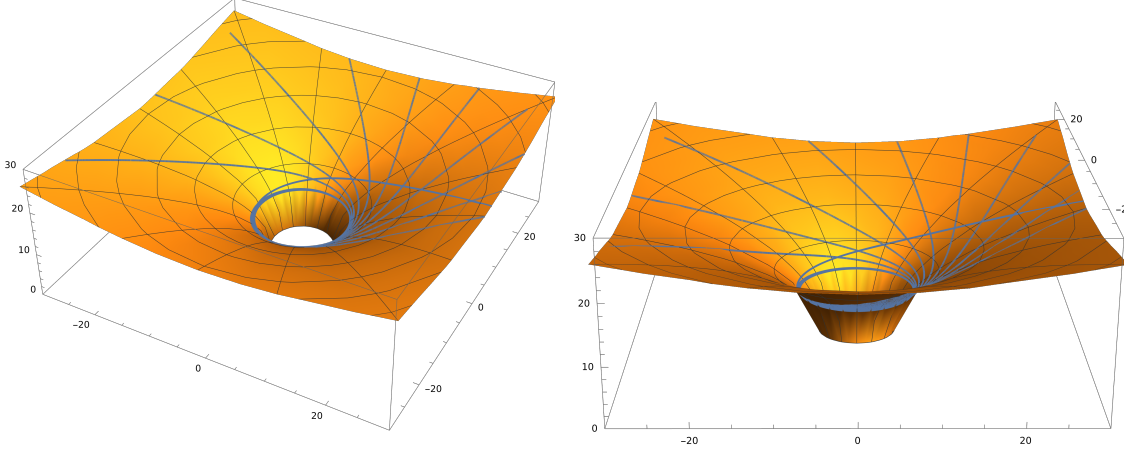


FIG. 2: Two views of the simulated light ray trajectories forming photon rings embedded into the Euclidean 3-space for a NUT hole with $l = m = 2$.

with $m = l = 2$ in table II.

V. RAY-TRACING ON EMBEDDING DIAGRAM

Here we digress from the discussion on the metamaterial analog of photon rings to show how one can acquire a better visualization of these rings by embedding them into the Euclidean 3-space. To this end we employ the embedding of the equatorial plane of NUT spacetime into the 3-dimensional Euclidean space with the following metric in cylindrical coordinates [25],

$$ds^2 = dZ^2 + dR^2 + R^2 d\phi^2, \quad (30)$$

in which, from the angular part of the NUT metric (1), we have $R^2 = r^2 + l^2$. It is shown that the usual embedding procedure will lead to the following embedding function $Z = Z(R)$ [25],

$$Z(R) = \int_{R_H}^R \left(\frac{3l^2 \tilde{R}^2 + 2m(\tilde{R}^2 - l^2)^{3/2} - 2l^4}{(\tilde{R}^2 - l^2)[\tilde{R}^2 - 2l^2 - 2m(\tilde{R}^2 - l^2)^{1/2}]} \right)^{1/2} d\tilde{R}. \quad (31)$$

where the result of integration is valid for $R > R_H = (r_H^2 + l^2)^{1/2}$. Now to find the light ray on the embedding diagram we only need to assign the extra $Z[R(\rho)]$ -dimension (obtained from the above integral and, written in terms of the isotropic radius) to any point on the ray with the isotropic radius ρ . The result of ray-tracing simulation on the embedding diagram of a NUT hole with $l = m = 2$ is depicted in Fig.2 for a congruence of 10 rays. These figures

show clearly how the light rays wrap around the throat of the embedding diagram at the radial location of the photon ring.

Having the above visualization of the photon rings, one should be careful not to associate the structure of our metamaterial analog of the equatorial NUT hole with the above embedding diagram. Indeed our metamaterial analog of the equatorial NUT hole is a flat 2-dimensional surface with the index of refraction adapted from the NUT spacetime geometry, and this is different from those studies in which spatially curved metamaterials are considered [26–28]. These studies necessitate the use of structured metamaterials with curved geometries to achieve an effective refractive index capable of facilitating light-trapping orbits.

VI. METAMATERIAL ANALOG OF A CHARGED NUT HOLE AS AN OPTICAL DEVICE: WAVE OPTICS APPROACH

It was noticed in the above simulations that m and l are just two parameters in the metamaterial’s isotropic index of refraction Eq. (25). Since the metamaterial analog of a NUT hole has two different parameters (m and l), one has more control over the design of the corresponding metamaterial with the required optical characteristics, as compared to the metamaterial analog of the pure NUT hole which has only one parameter. Utilizing unstable photon rings in metamaterials for the design of optical devices, such as an optical switch, this variety of parameters will allow designers to fine-tune the optical characteristics of the device with enhanced precision.

On the other hand, since in our approach, based on the spacetime index of refraction, we can perform an exact ray tracing simulation in the analog metamaterial, by adjusting the winding number of the photon ring, one can significantly increase the sensitivity of the device. This is achieved by increasing the critical angle’s precision in the simulation, as detailed in Table II.

In light of these considerations, this section will focus on the *charged* NUT solution, and its equatorial metamaterial analog associated with the spacetime’s index of refraction which contains three parameters. The charged NUT spacetime is an exact solution of the Einstein-Maxwell equations, which is obviously not a vacuum solution. It is noticed that its exotic features, as in the case of NUT solution, all are rooted in its NUT factor.

In Schwarzschild-like coordinates its metric is given by the following line element [18],

$$ds^2 = f(r)(dt - 2l \cos \theta d\phi)^2 - \frac{dr^2}{f(r)} - (r^2 + l^2)d\Omega^2, \quad (32)$$

with

$$f(r) = \frac{r^2 - 2mr - l^2 + q^2}{r^2 + l^2}, \quad (33)$$

in which m , l and q are the mass, NUT parameter, and the electric charge respectively. Applying the same procedure used in section III, one can show that the equivalent index of refraction for the equatorial charged NUT is given by,

$$n_{\text{CNUT}}(\rho) = \frac{1}{4} \frac{l^4 + 2l^2(m^2 + 4m\rho - q^2 + 12\rho^2) + (m - q + 2\rho)^2(m + q + 2\rho)^2}{\rho^2(q^2 + 4\rho^2 - l^2 - m^2)}. \quad (34)$$

Its detailed derivation is outlined in the appendix A. This three-parameter refractive index enhances the design flexibility of the corresponding metamaterial analog, offering more options for the placement of the analogs of the horizon and the photon ring within the optical device.

In the previous sections, we have used geometric optics, and ray-tracing simulation to investigate the optical properties of the metamaterial analog of the equatorial NUT spacetime. In this section, we employ wave optics to study the wave behavior of a metamaterial designed with the above index of refraction as a simple optical device.

To this end we look for a numerical solution of the Maxwell equations for wave propagation in an inhomogeneous dielectric medium. For our purposes, we assume that the matter is non-magnetic with the index of refraction $n(\rho) = c\sqrt{\mu_0 \epsilon(\rho)}$. By combining two of the Maxwell equations, we arrive at the following equation,

$$\nabla \times \nabla \times \mathbf{E} + \frac{n^2(\rho)}{c^2} \frac{\partial^2 \mathbf{E}}{\partial t^2} = 0. \quad (35)$$

To replicate the optical behavior of the spacetime of a charged NUT hole in a metamaterial device with the refractive index (34), we substitute $n_{\text{CNUT}}(\rho)$ for $n(\rho)$. Fig. 3 displays the results of numerical simulations for an electric dipole radiating in a medium with refractive index (34). These include two different cases with two different sets of parameters m, l, q : I) $m = 2 \times 10^{-6}, l = q = 0$ (the Schwarzschild case, Figs. 3a-3b), and II) $l = 2 \times 10^{-6}, m = q = 0$ (pure NUT case, Figs. 3c-3d). Figs. 3b and 3d) are the same as Figs. 3a and 3c) respectively, but with higher resolution around their corresponding analog horizons. As radiation traverses the metamaterial medium, it curves inward towards the central region, mimicking

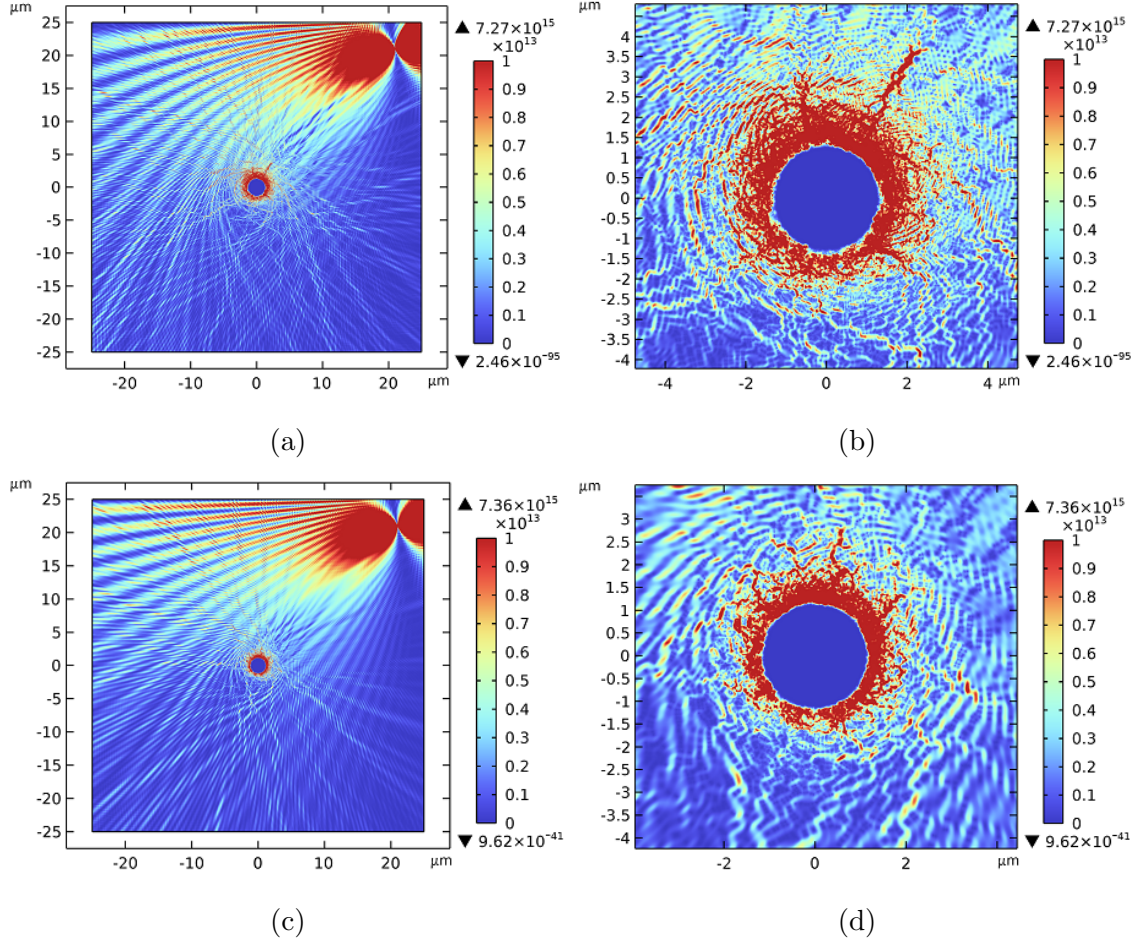


FIG. 3: Density plot of the electromagnetic radiation power from an electric dipole at a frequency of $f = 5.9958$ GHz in a metamaterial simulating 1)-Schwarzschild spacetime: (a) and (b), and 2) a pure NUT spacetime: (c) and (d). The event horizons form at $M/2$, $l/2$, and the photon rings form at $M/2(2 + \sqrt{3})$, $l/2(\sqrt{2} + \sqrt{3})$ for Schwarzschild and pure NUT cases, respectively.

the behavior of light passing by a massive object, and close to the photon ring position, revolves around the core in nearly-circular orbits.

In a few studies, including [10]-[11], Gaussian beams are utilized to explore the wave properties of analog materials. In these studies $r = 0$ is taken as the singularity point for the proposed refractive index. This obviously does not work for black hole solutions of Einstein field equations. Conversely, Chen et al. [5] apply Gaussian beams and truncate their numerical analysis at $r = a$, aiming to more accurately represent a black hole's event horizon. The isotropic analysis presented in [6] employs the exact refractive index of the

Schwarzschild metric, revealing wave properties akin to those we have depicted in Figs. 3a and 3b, where even subtle ripples are discernible. Figure 3 also illustrates a concentration of electromagnetic radiation around the event horizon, confirming the anticipated analog effect of the spacetime curvature directing radiation inward towards the center. Despite the fundamental distinctions between wave optics and geometric optics, the findings presented in this section concur with the outcomes detailed in Section IV.

As pointed out previously, the interesting optical behavior of the metamaterial analog of a charged NUT spacetime, with its 3-parameter index of refraction, can be employed in designing novel optical devices. Fig. 4 clearly demonstrates that by manipulating the three parameters $\{m, l, q\}$, we gain a greater control over the profile of $n(\rho)$, allowing us to tailor it to specific experimental requirements, including the design of a required optical devices. Alternatively one can obtain the set of the 3 parameters $\{m, l, q\}$ required for a desired metamaterial device with a given set of locations for its analog horizon and photon ring, and the value of the refractive index at a given position. For example by locating the horizon and photon ring at $\rho_H = 0.5 \times 10^{-6}$, and $\rho_c = 2 \times 10^{-6}$, respectively, and setting the refractive index value $n(\rho_c) = 2$, a metamaterial device can be crafted with the parameters $m = 1.42 \times 10^{-7}$, $l = 1.54 \times 10^{-6}$ and, $q = 1.18 \times 10^{-6}$ ². Figure 5 demonstrates this metamaterial's optical response to the radiation from an electric dipole. This plot shows a good agreement on the formation of the analogs of the horizon, and the photon ring between the wave optics approach and the ray-tracing simulations carried out in previous sections. It can be seen that as we get closer to the horizon, refractive index (Orange dot-dashed line in Fig. 4) increases and works as a barrier for the radiations. To contextualize our findings in relation to prior research, it is essential to acknowledge that, in order to address the numerical complexities arising from the rapid increase in the profile $n(\rho)$, previous studies have proposed the use of an absorbing inner medium within the core. Specifically, references [5, 10] advocate a cutoff radius slightly smaller than the horizon's radius, coupled with the assumption of an imaginary absorption medium. This configuration effectively absorbs all incoming waves, thereby emulating the physical characteristics of a black hole's inner horizon. Consequently, the wave concentration observed near the horizon in our simulations

² For this specific set of parameters, the polynomial discriminant Δ is negative. As expected, among the three potential solutions of the photon ring equation only r_c (ρ_c) lies outside the horizon.

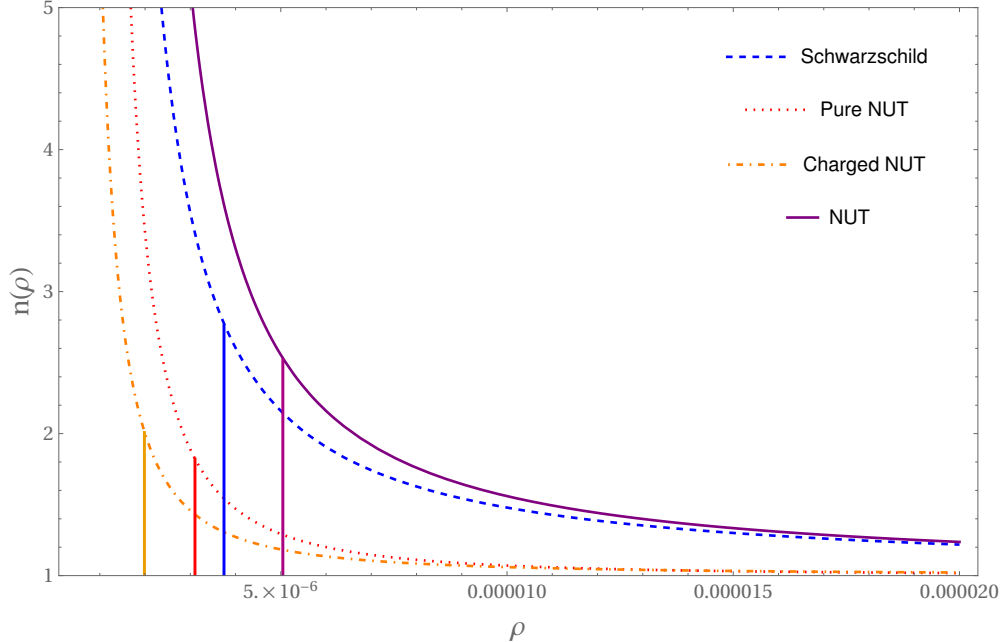


FIG. 4: Plots of function $n(\rho)$ for different members of the NUT family spacetimes, with vertical lines marking the positions of the photon rings.

does not occur in their configurations.

Careful consideration is required when selecting the parameters $\{m, l, q\}$ for a charged NUT-inspired metamaterial device, as the behavior of $n(\rho)$ is critical in our simulations. Theoretically, each parameter set determines a unique horizon position, denoted by (A11). As one approaches the horizon, $n(\rho)$ increases until diverges at the horizon. This phenomenon is illustrated in Fig. 4, where the behavior of the function $n(\rho)$ is depicted for four distinct cases of the NUT family spacetimes: Schwarzschild ($l = q = 0, m = 2 \times 10^{-6}$), Pure NUT ($m = q = 0, l = 2 \times 10^{-6}$), NUT ($m = l = 2 \times 10^{-6}, q = 0$), and the charged NUT ($m = 1.42 \times 10^{-7}, l = 1.54 \times 10^{-6}, q = 1.18 \times 10^{-6}$). The vertical lines in the plot mark the corresponding locations of photon rings at $\rho_c^{Sch} \simeq 3.732 \times 10^{-6}$, $\rho_c^{PNUT} \simeq 3.146 \times 10^{-6}$, $\rho_c^{NUT} \simeq 5.038 \times 10^{-6}$, and $\rho_c^{CNUT} \simeq 2 \times 10^{-6}$. These values are in agreement with the numerical solutions presented in Figs. 3 and 5. It should be emphasized that in order to achieve photon rings in optical devices, careful consideration of the value, and profile of $n(\rho)$ near the photon ring is essential. Indeed, a delicate computational meshing needs to be employed around these critical locations, and obviously leveraging a three-parameter refractive index facilitates this manipulation with a greater ease.

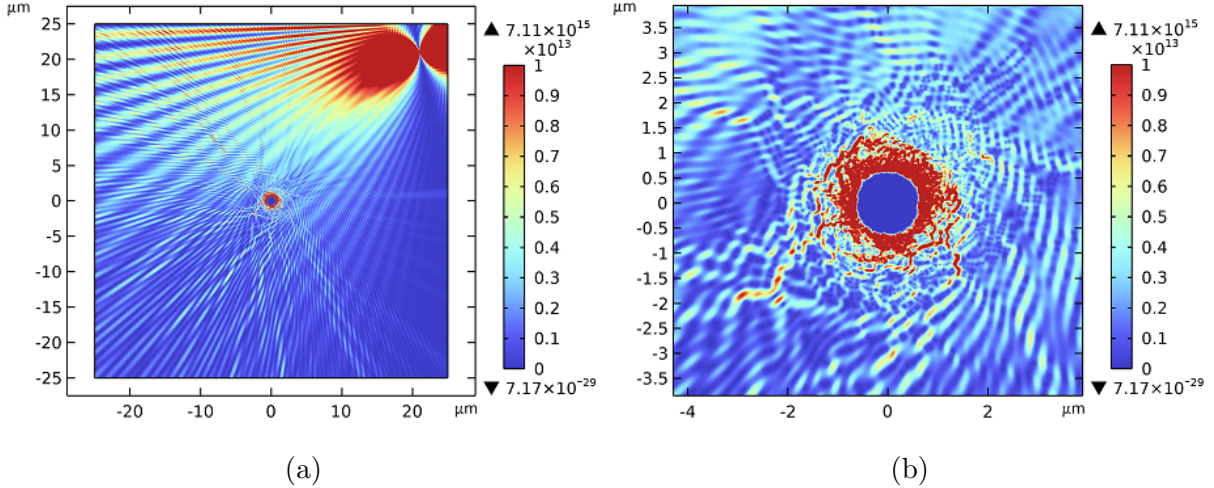


FIG. 5: Density plot of the electromagnetic radiation power from an electric dipole at a frequency of $f = 5.9958$ GHz in a metamaterial mimicking the charged NUT spacetime. Fig. (b) is the same as Fig. (a), but with a higher resolution around the analog horizon.

VII. CONCLUSIONS

Over the past few decades, analog spacetimes have attracted significant attention for their potential applications both in laboratory experiments and design of optical devices. This study explores the optical properties of the analogue spacetime associated with a gravitomagnetic monopole, a subject that has not been previously considered. We have investigated the null ray trajectories, and in particular the formation of photon rings in the metamaterial analogs of the equatorial NUT, and pure NUT spacetimes. To simulate light rays we have employed a previously introduced relation for the null rays in spherically symmetric spacetimes in their equatorial plane. In this study we have simulated the light ray trajectories in a 2-dimensional metamaterial which mimics the equatorial NUT, pure NUT and charged NUT spacetimes. Assigning a metamaterial with a refractive index identical to that of an equatorial NUT or pure NUT holes in isotropic coordinates, it was shown that the structure of light ray trajectories in these metamaterials exactly mimics that of the corresponding spacetime. This was explicitly shown for the case of photon rings in the metamaterial analogs of NUT and pure NUT holes.

One important observation from this two-parameter metamaterial analog is that, it enables us to identify the location of photon rings, without considerable change in the refractive

index, this observation can be confirmed by the provided plots. Clearly, as can be seen from $m = 0$, by changing l from 2 to 4, we would have a bigger photon ring, while we do not observe a significant change in the wavelength of the photons, i.e., the increase in the profile of $n_{\text{Pure-NUT}}(\rho)$ remains minimal. This observation can also be confirmed even for the case $m \neq 0$.

Most proposals for metamaterial analogs of black holes in the literature use an effective index of refraction and dielectric permittivity, which are not based on exact solutions of the Einstein field equations [9–11]. These proposals effectively mimic the light trajectories, but not the actual trajectories in the corresponding black hole geometry. On the other hand in [6], the authors employ a scalar refractive index assigned to the analogue medium of Schwarzschild spacetime.

In Refs. [26] and [27], a device made of a nematic liquid crystal, and hyperbolic metamaterial film on a catenoid was proposed. Their effective optical metric may or may not be a solution of the Einstein field equations. On the other hand, instead of using a 2-dimensional curved surface (such as a catenoid), here we propose design of 2-dimensional flat metamaterials endowed with refractive indices adapted from exact solutions of Einstein field equations, in which case the light rays in the metamaterial exactly mimic those in the corresponding spacetime. We also showed that by employing the same index of refraction in Maxwell's equation and solving them numerically in the wave optics limits, the results are compatible with ray-tracing simulations. Indeed from the figures 3 one could identify the approximate positions of the photon rings which are compatible with those obtained from the ray-tracing (geometric optics) simulation.

In the design of optical devices that replicate the optical characteristics of curved spacetimes, including black hole spacetimes, it is crucial to precisely control the refractive index profile as well as the positions of possible closed photon orbits (spheres and rings), and horizons due to experimental challenges. This level of control is more attainable with refractive indices having more than one parameter. In some previous studies [6, 11, 27] the authors made use of a one-parameter refractive index, while our study demonstrated that the three parameter index of refraction adapted from the charged NUT solution, provides enhanced control over the optical characteristics of its analogue metamaterial. This is particularly evident in the precise manipulation of the photon ring position, which could be instrumental in the design of advanced optical devices.

As a final comment, it is noted from the literature that there are two distinct motivations for investigating metamaterials with refractive indices adapted from black holes: I) To study the optical properties of black holes, as explored in references [5, 11], and II) To propose optical devices that exhibit unusual features of light, including light-trapping and slow-light capabilities [26, 29, 30]. Our simulations of the optical behaviour in the metamaterial analog of various NUT hole spacetime were conducted using indices of refraction represented by $n_{\text{NUT}}(\rho)$, $n_{\text{Pure-NUT}}(\rho)$ and $n_{\text{CNUT}}(\rho)$. These indices were approximated by a concentric circular mesh (with a constant index of refraction in each annulus), suggesting the feasibility of constructing such gradient-index optical analogs with conventional metamaterials. However, to obtain more accurate results, it is necessary to increase the number of annuli. This will provide a more precise simulation, and one could hope to gain a deeper understanding of the optical behavior in black hole geometries through their laboratory analogs, and on the metamaterial side, to explore potential avenues for developing novel metamaterial-based optical devices.

Acknowledgments

The authors would like to thank University of Tehran for supporting this project under the grants provided by the research council. They express their gratitude to the Department of Physics for granting access to its High-Performance Computing (HPC) system, as well as to the School of Physics at the Institute for Research in Fundamental Sciences (IPM) for providing access to its computational facilities. Additionally, they thank E. Kiani for his assistance with the Mathematica software. This work is based upon research funded by the Iran national science foundation (INSF) under the project No. 4005058.

Appendix A: Charged NUT hole

In this appendix, we derive the refractive index (34) for a charged NUT spacetime. We begin by substituting (33) into equation (13) to derive the equation for the photon ring,

$$(r_c^2 + l^2)^2 = (r_c^2 - 2mr_c - l^2 + q^2)b_c^2, \quad (\text{A1})$$

as the generalization of Eq. (15) in the presence of charge. By following the same procedure as in the NUT case, we can derive the equation governing the unstable circular photon

rings by taking the derivative with respect to r_c , which yields Eq. (16). Thus, the impact parameter b_c , will have the same relation as (17). After substituting b_c back into the equation (A1), we derive the following equation governing the position of the photon ring

$$r_c^3 - 3mr_c^2 - 3l^2r_c + 2q^2r_c + ml^2 = 0. \quad (\text{A2})$$

If the polynomial discriminant $\Delta = m^2(l^2 + m^2 - q^2)^2 - \frac{1}{27}(3l^2 + 3m^2 - 2q^2)^3$ is negative ($\Delta < 0$), all three roots are real and unequal with the following solutions

$$r_c = m + 2\sqrt{l^2 + m^2 - \frac{2q^2}{3}} \cos\left(\frac{1}{3}\tan^{-1}(\xi)\right), \quad (\text{A3})$$

$$r_c^\pm = m \pm \sqrt{l^2 + m^2 - \frac{2q^2}{3}} \left(\sqrt{3} \sin\left(\frac{1}{3}\tan^{-1}(\xi)\right) \mp \cos\left(\frac{1}{3}\tan^{-1}(\xi)\right) \right), \quad (\text{A4})$$

where

$$\xi = \frac{\sqrt{(3(l^2 + m^2) - 2q^2)^3 - 27m^2(l^2 + m^2 - q^2)^2}}{3\sqrt{3}m(l^2 + m^2 - q^2)}. \quad (\text{A5})$$

These solutions represent a generalization of the solutions given by equations (19) and (20), for the case of charged NUT spacetime. As in the NUT case, we observe that only the first solution yields a radius greater than the horizon r_H . Simultaneously, when $l = q = 0$, it reduces to the corresponding value for the photon ring in the Schwarzschild black hole, i.e., $r_{ps} = 3m$. However, the other two solutions, regardless of the values of l , m and q , lie inside the horizon and are not considered physically valid.

Therefore, the equatorial charged NUT spacetime in isotropic coordinates and its refractive index can be derived by applying the following coordinate transformation

$$r = \frac{(2\rho + m)^2 + l^2 - q^2}{4\rho}, \quad (\text{A6})$$

leading to

$$ds^2 = f(r(\rho)) dt^2 - F(\rho) dl_f^2, \quad (\text{A7})$$

$$f(r(\rho)) = \frac{(q^2 + 4\rho^2 - l^2 - m^2)^2}{l^4 + 2l^2(m^2 + 4m\rho - q^2 + 12\rho^2) + (m - q + 2\rho)^2(m + q + 2\rho)^2}, \quad (\text{A8})$$

$$F(\rho) = \frac{1}{\rho^2} \left[l^2 + \left(\left(\frac{l}{2\rho} \right)^2 - \left(\frac{q}{2\rho} \right)^2 + \left(1 + \frac{m}{2\rho} \right)^2 \right)^2 \right]. \quad (\text{A9})$$

The refractive index corresponding to the equatorial charged NUT can be expressed as,

$$n_{\text{RN-NUT}}(\rho) = \left[\frac{F(\rho)}{f(r(\rho))} \right]^{\frac{1}{2}} = \frac{1}{4} \frac{l^4 + 2l^2(m^2 + 4m\rho - q^2 + 12\rho^2) + (m - q + 2\rho)^2(m + q + 2\rho)^2}{\rho^2(q^2 + 4\rho^2 - l^2 - m^2)}, \quad (\text{A10})$$

Based on the given line element, the positions of the horizon, ρ_H , and the photon ring in isotropic coordinates are given by

$$\rho_H = \frac{1}{2} \sqrt{m^2 + l^2 - q^2}. \quad (\text{A11})$$

and

$$\begin{aligned} \rho_c = & \sqrt{l^2 + m^2 - \frac{2q^2}{3}} \cos\left(\frac{1}{3} \tan^{-1}(\xi)\right) \\ & + \frac{1}{2} \sqrt{\left((l^2 + m^2) - \frac{q^2}{3} + \left(2(l^2 + m^2) - \frac{4q^2}{3}\right) \cos\left(\frac{2}{3} \tan^{-1}(\xi)\right)\right)}, \end{aligned} \quad (\text{A12})$$

respectively. The impact parameter b_c for the rays forming the photon rings, is a constant of motion depending on the parameters m , l and q . It can be obtained by substituting the value of r_c from equation (A3) into equation (17).

-
- [1] D. R. Smith, J. B. Pendry and M. C. K. Wiltshire, *Science* **305**, 788 (2004); J. B. Pendry, D. Schurig and, D. R. Smith, *Science* **312**, 1780 (2006).
 - [2] U. Leonhardt, *Science* **312**, 1777 (2006).
 - [3] M. Nouri-Zonoz, A. Parvizi and H. Forghani-Ramandy, *Phys. Rev. D*, **106**, 124013 (2022).
 - [4] A. Greenleaf, et al., *Phys. Rev. Lett.*, **99**, 183901 (2007).
 - [5] H. Chen, R.-X. Miao, and M. Li, *Opt. Express*, **18**, 15183 (2010).
 - [6] I. Fernández-Núñez and O. Bulashenko, *Phys. Lett. A* **380**, 1 (2016).
 - [7] S. Maslovski, et al., *Phys. Rev. B*, **98**, 245143 (2018).
 - [8] R. A. Tinguely and A. P. Turner, *Commun. Phys.* **3**, 120 (2020).
 - [9] U. Leonhardt and P. Piwnicki, *Phys. Rev. Lett.*, **84**, 5 (2000).
 - [10] E. E. Narimanov and A. V. Kildishev, *Appl. Phys. Lett.* **95**, 041106 (2009).
 - [11] D. A. Genov, Shuang Zhang, and Xiang Zhang, *Nature Physics* **5**, 9 : 687-692 (2009).
 - [12] E. Newmann, L. Tamburini, and T. Unti, *J. Math. Phys.*, **4**, 915 (1963).
 - [13] C. W. Misner, *J. Math. Phys.* **4**, 924 (1963).
 - [14] C. W. Misner, University of Maryland, Department of Physics and Astronomy, Report number : MDDP-TR-529 (1965).
 - [15] S. Chandrasekhar, *The mathematical theory of black holes*, Oxford University Press (1986).

- [16] F. dos Santos Azevedo, et al., Europhysics Letters 124.3 (2018): 34006.
- [17] Y. Rosenberg, Philosophical Transactions of the Royal Society A **378**, 2177 (2020).
- [18] H. Stephani, D. Kramer, M. MacCallum, C. Hoenselaers, E. and Herlt, *Exact Solutions of Einstein's Field Equations*, Cambridge University Press (2003).
- [19] J. G. Miller, M. D. Kruskal and B. B. Godfrey, Phys. Rev. D **4**, 2945 (1971).
- [20] M. Demianski and E. T. Newman, Bull. Acad. Pol. Sci. Ser. Sci. Math. Astron. Phys., **14**, 653 (1966).
- [21] D. Lynden-Bell and M. Nouri-Zonoz, Rev. Mod. Phys., **70**, 427 (1998).
- [22] W. B. Bonnor, Proc. Camb. Phil. Soc., **66**, 145 (1969).
- [23] R. L. Zimmerman and B. Y. Shahir, General Relativity and Gravitation, **21**, No. 8, 1989.
- [24] M. Nouri-Zonoz and D. Lynden-Bell, Mon. Not. R. Astron. Soc., 292(3):714–722, (1997).
- [25] H. Sadegh, E. Kiani, and M. Nouri-Zonoz, arXiv:2308.03104 (2023).
- [26] F. dos Santos Azevedo, et al. Phys. Rev. A, **103** (2), 023516 (2021).
- [27] F. dos Santos Azevedo, et al., Europhysics Letters 137 (4), 45001 (2022).
- [28] V. Atanasov, R. Dandoloﬀ, and A. Saxena, Physica Scripta, **96**, 12 (2021).
- [29] D. Schurig et al., Science **314**, 5801 (2006).
- [30] M. Manjappa et al., Applied Physics Letters **106**, 18 (2015).